Comprehensive Investigation of Statistical Effects in Nitride Memories—Part I: Physics-Based Modeling

Aurelio Mauri, Christian Monzio Compagnoni, *Member, IEEE*, Salvatore Maria Amoroso, Alessandro Maconi, Andrea Ghetti, *Member, IEEE*, Alessandro S. Spinelli, *Senior Member, IEEE*, and Andrea L. Lacaita, *Fellow, IEEE*

***Abstract*—This paper presents a comprehensive investigation of statistical effects in deeply scaled nitride memory cells, considering both atomistic substrate doping and the discrete and localized nature of stored charge in the nitride layer. By means of 3-D TCAD simulations, the statistical dispersion of the threshold voltage shift induced by a single localized electron in the nitride is evaluated in presence of non-uniform substrate conduction. The role of 3-D electrostatics and atomistic doping on the results is highlighted, showing the latter as the major spread source. The threshold voltage shift induced by more than one electron in the nitride is then analyzed, showing that for increasing numbers of stored electrons a correlation among single-electron shifts clearly appears. The scaling trend and the practical impact of these statistical effects on cell operation are discussed in Part II of this paper.**

***Index Terms*—Atomistic doping, nitride memories, semiconductor device modeling, SONOS memories, TANOS memories.**

I. Introduction

SONOS and TANOS memories are considered today the most practical evolution of the floating-gate (FG) NAND Flash technology, allowing improved reliability thanks to discrete charge storage in thin silicon nitride layers [1]–[8]. To investigate their performance, many 1-D models have been reported to describe the charging/discharging dynamics of relatively large area cells and capacitors [9]–[13]. However, all these models suffer from two main limitations that question their validity for the investigation of decananometer-sized memory cells, i.e., the lack of 1) the real 3-D cell electrostatics during program/erase (P/E) and read and 2) the discrete and localized nature of stored electrons. Considering 3-D electrostatics is mandatory to account for fringing fields at the active area edges, determining both a non-uniform charge injection to/from the nitride layer during P/E and non-uniform substrate inversion during read [14], [15]. In this context, the correct evaluation of the threshold voltage shift (ΔV_T) determined by the discrete and localized electrons stored in the nitride after program requires a careful numerical simulation of source/drain conduction during read. Moreover, the discrete nature of the stored charge necessarily gives rise to statistical issues related to the number and position fluctuation of the electrons in the nitride, determining a statistical dispersion of ΔV_T after program which cannot be investigated by any 1-D model. This statistical dispersion is further worsened when considering the additional contribution of atomistic doping to non-uniform substrate inversion, enhancing percolative source-to-drain conduction [16]–[20].

In this paper, we present a comprehensive 3-D numerical investigation of decananometer-sized nitride memory cells, considering both atomistic substrate doping and discrete and localized electron storage in the nitride. To correctly capture the stored charge effect, not only on substrate inversion but also on source-to-drain conduction, ΔV_T is evaluated from cell drain current–gate voltage $(I_D$–$V_G)$ transcharacteristics, obtained solving the transport equations in the active area. By means of Monte Carlo simulations, the statistical distribution of the threshold voltage shift induced by a single localized electron randomly placed in the nitride volume $(\Delta V_{T,1})$ is evaluated, accounting for dopant number and position randomness in the substrate. The role of 3-D electrostatics and atomistic doping on the $\Delta V_{T,1}$ distribution is highlighted, showing the latter as the major spread source. Then, the threshold voltage shift induced by N electrons stored in the nitride $(\Delta V_{T,N})$ is analyzed, showing that for large N a correlation among single-electron shifts clearly appears, reducing the spread of the $\Delta V_{T,N}$ distribution. The impact of these results on the program operation of deeply scaled nitride-based cells is investigated in the companion paper [1], where a scaling analysis is also presented.

II. Physics-Based Numerical Model

We performed 3-D TCAD simulations on the template device structure reported in Fig. 1, featuring: STI trenches at the cell sides, atomistic doping in the substrate and discrete electrons in the nitride layer. A bottom oxide/nitride/top oxide (ONO) stack with thicknesses equal to 4/4.5/5 nm was assumed for the gate dielectric, with the nitride layer patterned over cell channel ($\epsilon_{\rm ox} = 3.9$ and $\epsilon_N = 7.5$ were used for the relative dielectric constants of silicon oxide and nitride, respectively). Cell width (W) and length (L) were set to 25 nm, with a constant substrate

Manuscript received February 17, 2010; revised April 30, 2010; accepted June 14, 2010. Date of publication July 26, 2010; date of current version August 20, 2010. This work was supported by the European Commission through the "GOSSAMER" Project under FP7 Research Contract 214431. The review of this paper was arranged by Editor S. Deleonibus.

A. Mauri and A. Ghetti are with Numonyx, R&D—Technology Development, 20041 Agrate Brianza (MI), Italy.

C. Monzio Compagnoni, S. M. Amoroso, and A. Maconi are with the Dipartimento di Elettronica e Informazione, Politecnico di Milano, 20133 Milano, Italy, and also with the Italian University Nano-Electronics Team, 40125 Bologna, Italy.

A. S. Spinelli and A. L. Lacaita are with the Dipartimento di Elettronica e Informazione, Politecnico di Milano, 20133 Milano, Italy, with the Italian University Nano-Electronics Team, 40125 Bologna, Italy, and also with the Istituto di Fotonica e Nanotecnologie—Consiglio Nazionale delle Ricerche, 20133 Milano, Italy.

Color versions of one or more of the figures in this paper are available online at http://ieeexplore.ieee.org.

Digital Object Identifier 10.1109/TED.2010.2054472

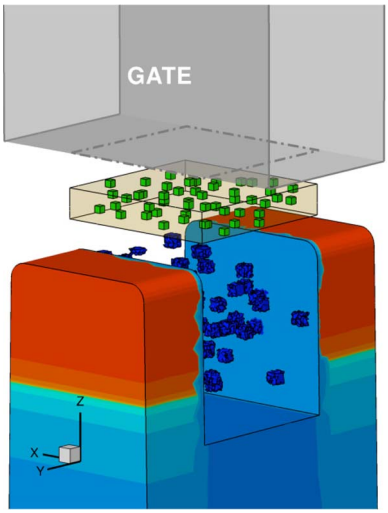

Fig. 1. Schematics for the cell structure investigated in this work, highlighting the atomistic doping region in the substrate and the discrete localized electrons stored in the nitride. The gate dielectric comprises an oxide/nitride/oxide (ONO) stack. Red regions: n implants; blue regions: p substrate; green regions: nitride; oxide regions are not highlighted.

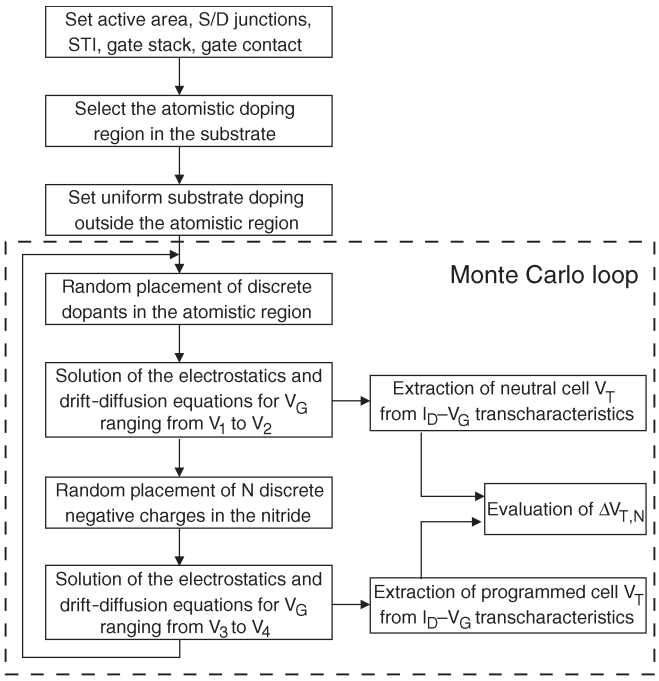

Fig. 2. Block diagram for the simulation procedure used to collect statistical information on $V_{T,0}$ and $\Delta V_{T,N}$. $V_{G,1}$, $V_{G,2}$, $V_{G,3}$ and $V_{G,4}$ define the explored V_G ranges for the neutral and programmed cell state.

doping $N_a = 3 \times 10^{18}$ cm^{-3}. A planar metal word-line was assumed for the gate [14].

The simulation flow is schematically depicted in Fig. 2. After the definition of the template device structure, the atomistic doping region in the substrate was set with a depth from the substrate/oxide interface (25 nm) larger than the average depletion layer width at threshold. Outside this region, a continuous doping profile was used. A Monte Carlo loop was employed to collect statistical information on the cells. The loop includes the extraction of the actual number of dopants in the discretization region from a Poisson statistics with average value $N_a^d = 46$ (as resulting from the product of N_a and the volume of doping discretization) and their placement according to a uniform distribution. Poisson and drift–diffusion equations were then solved for fixed drain bias $V_D = 0.7$ V (source and bulk grounded) and increasing gate bias to obtain the I_D–V_G transcharacteristics. This was then used to extract neutral cell threshold voltage $(V_{T,0})$ as the gate bias allowing 200 nA to flow from source to drain. I_D–V_G and V_T were then calculated again after a fixed number N of electrons were randomly placed in the nitride volume to investigate the programmed cell state, extracting $\Delta V_{T,N}$. More than 100 Monte Carlo runs were used to obtain the $V_{T,0}$ and $\Delta V_{T,N}$ statistics. Note that the maximum number of Monte Carlo runs has to be considered when defining the thickness of the atomistic doping region, for the cell with the lower number of dopants out of the Poisson statistics to have a depletion layer completely included in this region.

All the simulations were performed by means of a commercial software [21], implementing in its framework the tools to deal with atomistic substrate doping and discrete electron placement in the nitride. To this aim, we followed a simulation approach similar to what is reported in [22], using a constant mobility value for the drift–diffusion simulations [18], [22] and spreading the dopant charge in a cube of side equal to 2 nm centered in the chosen atomistic dopant position. The cube side was selected from the compromise between a better resolution of percolative substrate conduction and the necessity to avoid artificial charge localizations when solving the poisson and drift–diffusion equations in presence of Coulomb potential wells, as discussed in detail in [18]. This compromise could be fully solved only by more complex simulation approaches, such as introducing quantum-corrections to the electrostatic solution [18] or splitting the Coulomb potential into short- and long-range components [16]. Similarly, localized electron storage in the nitride was reproduced by placing the electronic charge in a cube of 1 nm side centered in each selected storage position.

III. $\Delta V_{T,1}$ Statistical Distribution

Fig. 3 shows the statistical distribution of $V_{T,0}$ obtained from the Monte Carlo simulation analysis presented in the previous section. Although current crowding at the cell corners determined by 3-D electrostatics impacts the average value $\overline{V_{T,0}} = 2$ V of the distribution, its broadening is the result of atomistic doping [17], [20]. In fact, substrate percolative conduction is determined by the number and position of dopants placed in the discretization region, with different cells showing different $V_{T,0}$ as a result of a more or less favorable configuration of doping atoms from the source-to-drain conduction standpoint. Note that the resulting $V_{T,0}$ statistics in Fig. 3 displays a good Gaussian behavior, with a standard deviation $\sigma = 195$ mV.

We began our investigation of the programmed cell state by considering a single trapped electron (i.e., $N = 1$) randomly placed in a localized position inside the nitride volume. The statistical distribution of the V_T shift obtained with respect to the neutral cell state $(\Delta V_{T,1})$ is shown in Fig. 4 (solid line), displaying an average value of $\overline{\Delta V_{T,1}} = 22$ mV and a standard deviation $\sigma_{\Delta V_{T,1}} = 8.5$ mV. Moreover, a clear exponential tail

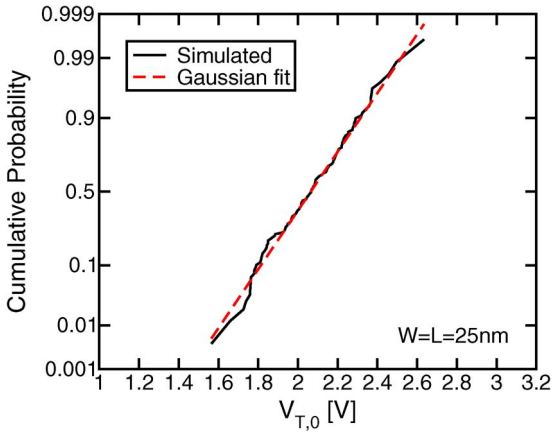

Fig. 3. Simulated statistical distribution of V_T for neutral (no charge in the nitride) cells.

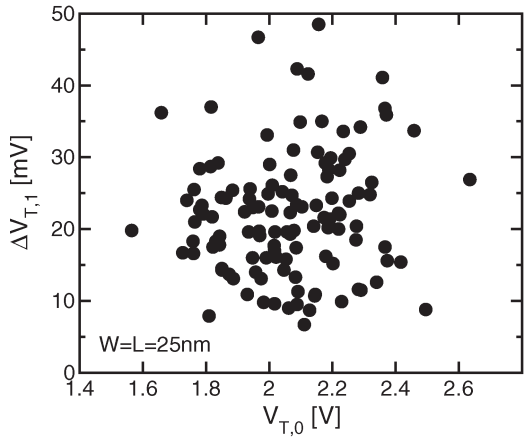

Fig. 5. Simulated $\Delta V_{T,1}$ as a function of cell $V_{T,0}$, considering 3-D electrostatics and atomistic substrate doping.

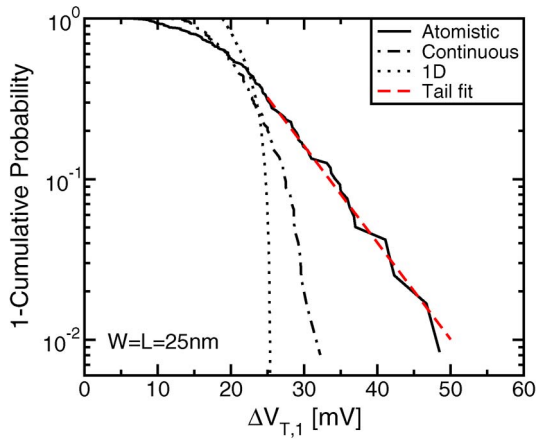

Fig. 4. Simulated statistical distribution of the threshold voltage shift determined by one localized electron randomly placed in the nitride volume.

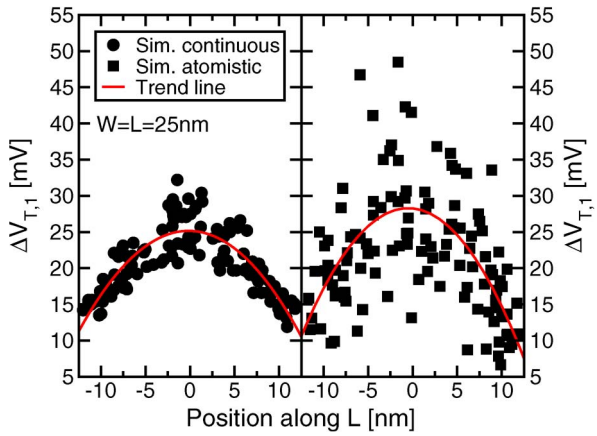

Fig. 6. $\Delta V_{T,1}$ as a function of the electron position along L for the case of continuous (left) and atomistic (right) substrate doping. 0 is the channel center.

departs in the positive $\Delta V_{T,1}$ direction, which means that single electrons can result into very large V_T shifts, though with low probabilities. Note that this behavior cannot be predicted by any 1-D model. In fact, in a 1-D treatment, the only spread source for $\Delta V_{T,1}$ is the vertical position of the stored electron in the nitride layer. This affects the V_T shift according to $\Delta V_{T,1}^{\text{1-D}} = -q'(t_2/\epsilon_{ox} + t_x/\epsilon_N)$, where $q' = q/WL$ is the electron charge normalized to cell area and t_2 is the top oxide thickness. Assuming a random distance t_x of the electron from the nitride/top oxide interface, the resulting 1-D distribution of $\Delta V_{T,1}$ is reported in Fig. 4 (dots). The distribution has been calculated including a scaling factor equal to 2.09 to the $\Delta V_{T,1}^{\text{1-D}}$ values to obtain the same average result given by 3-D simulations, as will be explained in the companion paper [1]. Note that this distribution is much tighter than what is predicted by the accurate 3-D analysis, revealing a dominant contribution of 3-D electrostatics and random dopant effects on the $\Delta V_{T,1}$ statistics.

To separate the contribution of atomistic doping and 3-D electrostatics to the statistical dispersion of $\Delta V_{T,1}$, Fig. 4 also shows results obtained for continuous substrate doping (dashed–dotted line). This distribution highlights the effect of a single, localized electron in the nitride on source-to-drain conduction, correctly taking into account 3-D electrostatics but neglecting the contribution of atomistic doping to non-uniform substrate inversion. The lower statistical dispersion of $\Delta V_{T,1}$ with respect to the case when atomistic doping is accounted for reveals that percolative source-to-drain conduction has a major role in determining the impact of a single trapped electron on V_T, and that this is strongly affected by the discrete nature of substrate dopants. However, Fig. 5 makes clear that there is no correlation between $V_{T,0}$ and $\Delta V_{T,1}$.

To better understand the results of Fig. 4, we reported the $\Delta V_{T,1}$ values as a function of the electron position along L, W, and nitride thickness t_N in Figs. 6–8 for the case of continuous (left) and atomistic (right) substrate doping. Results of Figs. 6 and 7 are similar to what was already obtained for the case of random telegraph noise (RTN) in Flash devices [20], [23]: the V_T shift is larger when the electron is placed half-way between source and drain, due to a more effective electrostatic control of channel inversion, or close to the edges along W, due to the possibility for the electron to stop a larger part of drain current, as field intensification at the edges locally increases the inversion charge and the drain current density. Fig. 8 then reveals the average increase of $\Delta V_{T,1}$ when the electron is moved closer to the nitride/bottom oxide interface, as also predicted by 1-D electrostatics.

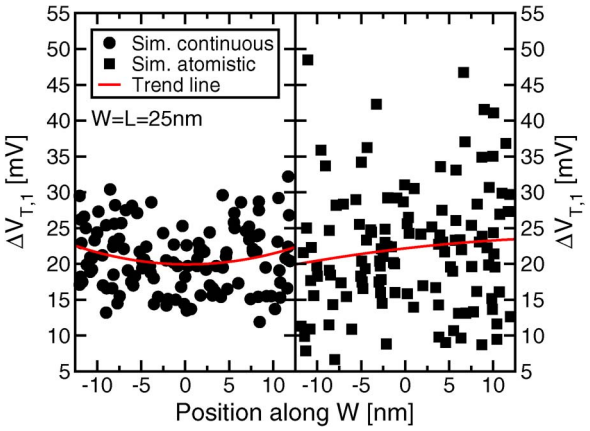

Fig. 7. Same as Fig. 6 but as a function of the electron position along W. 0 is the channel center.

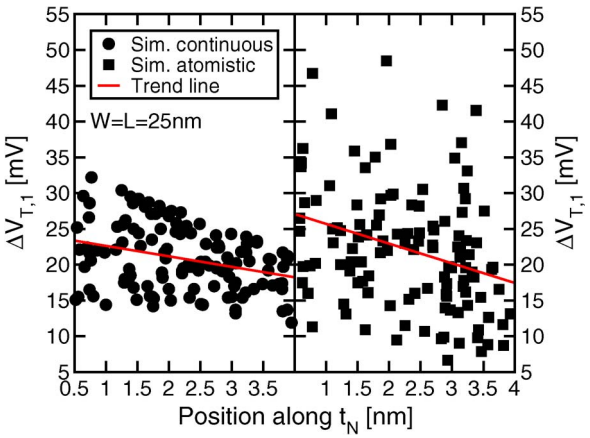

Fig. 8. Same as Fig. 6 but as a function of the electron position along t_N. 0 is the nitride/bottom oxide interface.

Superimposed on the average trend is the statistical dispersion of the results, due to fluctuations in the electron position (e.g., in Fig. 6 the spread is due to fluctuations along W and t_N). In particular, in Fig. 8 the $\Delta V_{T,1}$ spread reduces when the electron is placed closer to the top oxide. This is ascribed to a less-local electrostatic effect of the stored electron on the substrate when the distance between electron and substrate grows, reducing the impact of non-uniformities in the current density profile. In the case of atomistic doping, a larger dispersion of $\Delta V_{T,1}$ can be seen in Figs. 6–8, which was already evident in Fig. 4. For our simulation set, this increased spread totally overrides the weak average W dependence of $\Delta V_{T,1}$ that was shown by the continuous doping results (see the different trend lines). The origin of this additional spread is obviously the enhancement of percolative conduction determined by atomistic doping, resulting into a statistical dispersion of $\Delta V_{T,1}$ that is larger than that given by 3-D electrostatics alone. In fact, atomistic doping enhances the possibility to have cells where source-to-drain current takes place along few strong percolation paths, allowing a single electron to largely block cell conduction when this is exactly placed over a path where current crowding occurs [20], [24]–[26]. In this case, quite a large V_T shift results, contributing to the enlargement of the $\Delta V_{T,1}$ statistics.

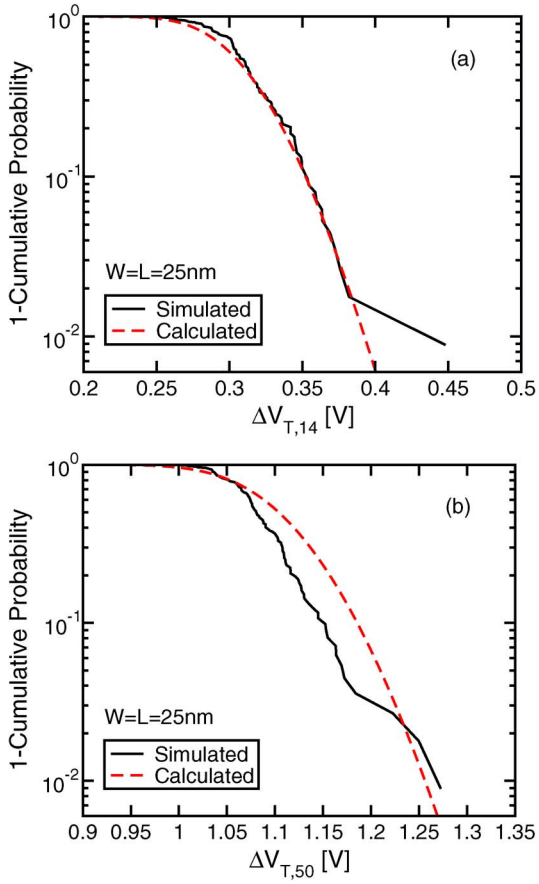

Fig. 9. Simulated $\Delta V_{T,N}$ distribution in the case of (a) $N = 14$ and (b) 50 electrons stored in the nitride layer (black lines). Red dashed lines represent the calculated distributions assuming independent trap superposition and the $\Delta V_{T,1}$ distribution of Fig. 4.

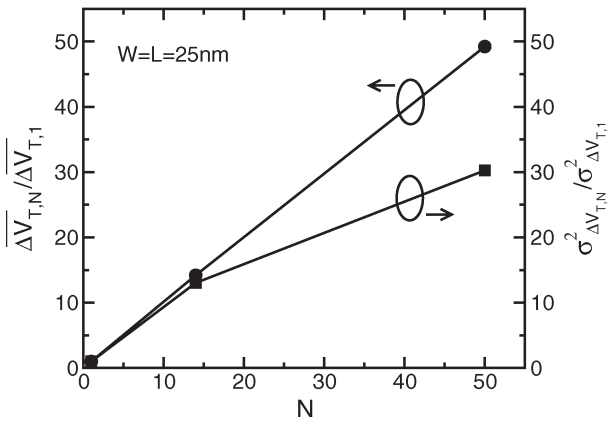

Fig. 10. Normalized average and variance of $\Delta V_{T,N}$ as a function of the number of electrons stored in the nitride.

IV. $\Delta V_{T,N}$ Statistical Distribution

To investigate how multiple electrons combine their effect to determine the V_T shift, we ran Monte Carlo simulations with $N > 1$. Electrons were placed randomly in the nitride volume according to a uniform distribution, therefore neglecting any disuniformity in the stored charge profile after program that may arise from a non-uniform injection field in the bottom oxide. Fig. 9 shows the statistical distributions of $\Delta V_{T,N}$ for the

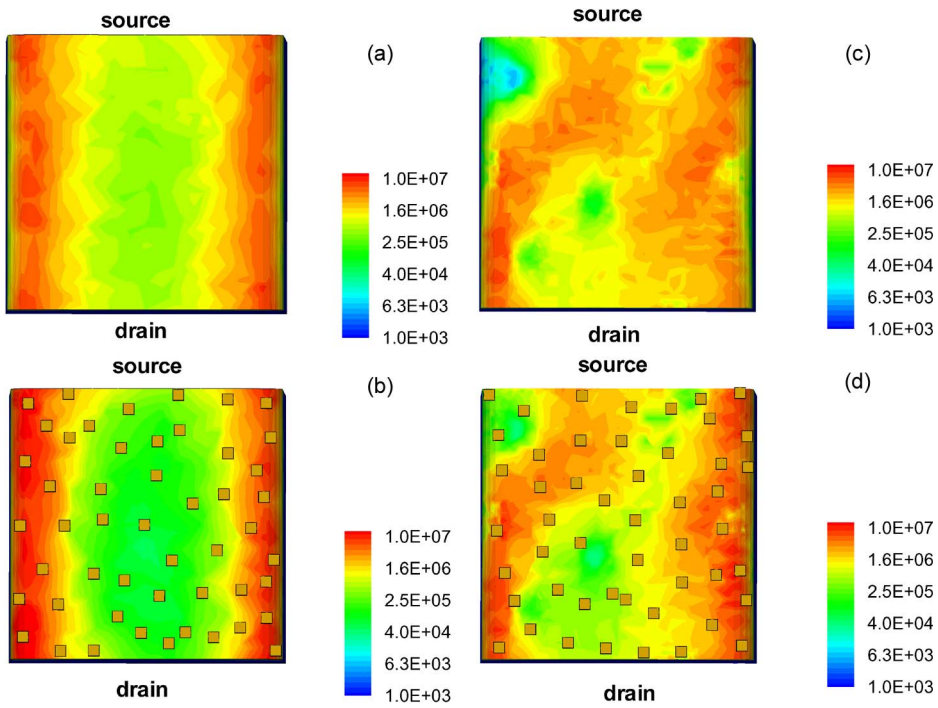

Fig. 11. Plot of the current density at threshold for: (a) continuous doping, neutral cell; (b) continuous doping, 50 electrons in the nitride; (c) atomistic doping, neutral cell; (d) atomistic doping, 50 electrons in the nitride. Small fluctuations along L in case (a) are due to numerical interpolations used to extract the current density profile at the substrate surface.

case of $N = 14$ and 50. A larger statistical dispersion of $\Delta V_{T,N}$ appears with respect to the case of $N = 1$, contradicting the 1-D prediction of a spread reduction due to a more stable charge centroid in presence of a larger number of electrons in the nitride. To further investigate this point, Fig. 9 also shows the $\Delta V_{T,N}$ distribution calculated from $N - 1$ self-convolutions of the $\Delta V_{T,1}$ statistics (red dashed lines). This distribution is expected to describe the $\Delta V_{T,N}$ statistics in case electrons add their individual contribution to the V_T shift independently one another. The predicted curve is in good agreement with the simulated $\Delta V_{T,N}$ distribution in the case of $N = 14$, revealing a statistically independent effect of the stored electrons on V_T for small N. However, this is no longer true for $N = 50$, where non-negligible differences appear between simulation results and calculations, highlighting a correlation among the stored electrons effect on V_T. This can be clearly seen from Fig. 10, where the average value and variance of $\Delta V_{T,N}$ ($\overline{\Delta V_{T,N}}$ and $\sigma^2_{\Delta V_{T,N}}$, respectively) are shown normalized to the average value and variance of $\Delta V_{T,1}$ ($\overline{\Delta V_{T,1}}$ and $\sigma^2_{\Delta V_{T,1}}$) as a function of N. While the relation $\overline{\Delta V_{T,N}} = N \times \Delta V_{T,1}$ correctly holds, $\sigma^2_{\Delta V_{T,N}}$ equals $13.03\times$ and $30.26 \times \sigma^2_{\Delta V_{T,1}}$, respectively for $N = 14$ and $N = 50$. This result confirms that stored electrons act independently for low N, thanks to the large distance among them. However, when their mutual distances decrease, their positions get closer and the spread is reduced due to their correlated electrostatic control on substrate inversion.

Further insight can be obtained from the plots of the current density at threshold shown in Fig. 11. The left column refers to continuous doping for neutral (top) and programmed (bottom) cell; the right column is analogous but related to a case of atomistic doping. Results for continuous doping and neutral cell clearly show the non-uniform current density profile in the substrate determined by field enhancement at the cell corners, locally increasing the inversion charge. A different current density profile is instead present in the case of atomistic doping, due to the additional and random effect of discrete dopants on substrate inversion. However, in both cases, dicrete and localized electrons in the nitride slightly modify the current density profile in the substrate, due to the local nature of the electrostatic effect of each electron on substrate inversion. In this framework, the effect of stored electrons on substrate conduction is similar to that of atomistic doping, introducing randomness in the percolation paths connecting source-to-drain at threshold. Moreover, this means that a different current density profile is present in the substrate for neutral and programmed cells, changing, for instance, the impact on V_T of a single electron trapped in the bottom oxide. This point will be further discussed in the companion paper [1], where RTN in nitride cells will be addressed in detail.

V. Discussion

Although the quantitative data obtained so far refer to the particular device structure investigated and should be cautiously applied to different (e.g., non-planar) cell geometries [14], the picture emerging from Figs. 4 and 9 is that of a significant V_T spread following electron injection. Such a spread impacts the V_T control, which must be retained for all cells in the array, i.e., down to very low probability levels. For example, Fig. 4 shows that a single electron may give rise to a V_T shift of 50 mV with a probability of 10^{-2}, representing a high probability level for Flash arrays. This ΔV_T may, in turn, appear as a

V_T-loss during data retention, determining a critical reliability issue for multi-level devices, where a severe control of V_T is required. Moreover, the statistical dispersion of ΔV_T may also influence the P/E operation of these devices. In fact, due to the relatively small separation among the V_T levels, multi-level arrays usually adopt a staircase algorithm for the program operation, resulting into very tight programmed V_T distributions. The width of these distributions is limited by many different physical phenomena, among which electron injection statistics [27], [28] and RTN [29]–[33] represent severe reliability constraints. In the case of nitride memory cells, the $\Delta V_{T,N}$ statistical spread may give an additional contribution to the dispersion of the programmed V_T distribution, as will be discussed in detail in the companion paper [1], where a scaling analysis of the $\Delta V_{T,N}$ statistical distribution will also be presented.

VI. Conclusion

This paper presented a comprehensive investigation of statistical effects in deeply scaled nitride memory cells, highlighting that 3-D electrostatics, atomistic substrate doping, and charge localization in the nitride volume result into a statistical dispersion of ΔV_T. The local electrostatic effect of stored electrons and percolative substrate conduction were shown as the main reason for the ΔV_T spread. A scaling analysis and the investigation of the practical impact of these statistical results on cell operation are provided in the companion paper [1].

Acknowledgment

The authors would like to thank R. Gusmeroli from Politecnico di Milano, and P. Cappelletti, E. Camerlenghi, R. Bez, L. Baldi, and E. Greco from Numonyx for discussions and support.

References

[1] C. Monzio Compagnoni, A. Mauri, S. M. Amoroso, A. Maconi, E. Greco, and A. S. Spinelli, "Comprehensive investigation of statistical effects in nitride memories—Part II: Scaling analysis and impact on device performance," *IEEE Trans. Electron Devices*, vol. 57, no. 9, pp. 2124–2131, Sep. 2010.

[2] T. Y. Chan, K. K. Young, and C. Hu, "A true single-transistor oxide-nitride-oxide EEPROM device," *IEEE Electron Device Lett.*, vol. EDL-8, no. 3, pp. 93–95, Mar. 1987.

[3] J. Bu and M. H. White, "Design considerations in scaled SONOS nonvolatile memory devices," *Solid State Electron.*, vol. 45, no. 1, pp. 113–120, Jan. 2001.

[4] C. H. Lee, K. I. Choi, M. K. Cho, Y. H. Song, K. C. Park, and K. Kim, "A novel SONOS structure of $SiO_2/SiN/Al_2O_3$ with TaN metal gate for multi-giga bit flash memories," in *IEDM Tech. Dig.*, 2003, pp. 613–616.

[5] Y. Shin, J. Choi, C. Kang, C. Lee, K.-T. Park, J.-S. Lee, J. Sel, V. Kim, B. Choi, J. Sim, D. Kim, H.-J. Cho, and K. Kim, "A novel NAND-type MONOS memory using 63 nm process technology for multi-gigabit flash EEPROM," in *IEDM Tech. Dig.*, 2005, pp. 337–340.

[6] Y. Park, J. Choi, C. Kang, C. Lee, Y. Shin, B. Choi, J. Kim, S. Jeon, J. Sel, J. Park, K. Choi, T. Yoo, J. Sim, and K. Kim, "Highly manufacturable 32 Gb multi-level NAND flash memory with 0.0098 μm^2 cell size using TANOS (Si-Oxide- Al_2O_3-TaN) cell technology," in *IEDM Tech. Dig.*, 2006, pp. 29–32.

[7] J. S. Sim, J. Park, C. Kang, W. Jung, Y. Shin, J. Kim, J. Sel, C. Lee, S. Jeon, Y. Jeong, Y. Park, J. Choi, and W.-S. Lee, "Self aligned trap-shallow trench isolation scheme for the reliability of TANOS (TaN/AlO/SiN/Oxide/Si) NAND flash memory," in *Proc. Non-Volatile Semicond. Memory Workshop*, 2007, pp. 110–111.

[8] C.-H. Lee, J. Choi, C. Kang, Y. Shin, J.-S. Lee, J. Sel, J. Sim, S. Jeon, B.-I. Choe, D. Bae, K. Park, and K. Kim, "Multi-level NAND flash memory with 63 nm-node TANOS (Si-Oxide-SiN- Al_2O_3-TaN) cell structure," in *VLSI Symp. Tech. Dig.*, 2006, pp. 21–22.

[9] A. Paul, C. Sridhar, and S. Mahapatra, "Comprehensive simulation of program, erase and retention in charge trapping flash memories," in *IEDM Tech. Dig.*, 2006, pp. 393–396.

[10] A. Furnemont, M. Rosmeulen, A. Cacciato, L. Breuil, K. De Meyer, H. Maes, and J. Van Houdt, "A consistent model for SANOS programming operation," in *Proc. Non-Volatile Semicond. Memory Workshop*, 2007, pp. 96–97.

[11] E.-S. Choi, H.-S. Yoo, K.-H. Park, S.-J. Kim, J.-R. Ahn, M.-S. Lee, Y.-O. Hong, S.-G. Kim, J.-C. Om, M.-S. Joo, S.-H. Pyi, S.-S. Lee, S.-K. Lee, and G.-H. Bae, "Modeling and characterization of program/erasure speed and retention of TiN-gate MANOS (Si-Oxide- SiN_x-Al_2O_3-metal gate) cells for NAND flash memory," in *Proc. Non-Volatile Semicond. Memory Workshop*, 2007, pp. 83–84.

[12] C. Monzio Compagnoni, A. Mauri, S. M. Amoroso, A. Maconi, and A. S. Spinelli, "Physical modeling for programming of TANOS memories in the Fowler-Nordheim regime," *IEEE Trans. Electron Devices*, vol. 56, no. 9, pp. 2008–2015, Sep. 2009.

[13] E. Vianello, F. Driussi, A. Arreghini, P. Palestri, D. Esseni, L. Selmi, N. Akil, M. J. van Duuren, and D. S. Golubovic, "Experimental and simulation analysis of program/retention transients in silicon nitride-based NVM cells," *IEEE Trans. Electron Devices*, vol. 56, no. 9, pp. 1980–1990, Sep. 2009.

[14] H.-T. Lue, T.-H. Hsu, S.-Y. Wang, Y.-H. Hsiao, E.-K. Lai, L.-W. Yang, T. Yang, K.-C. Chen, K.-Y. Hsieh, R. Liu, and C.-Y. Lu, "Study of local trapping and STI edge effects on charge-trapping NAND flash," in *IEDM Tech. Dig.*, 2007, pp. 161–164.

[15] H.-T. Lue, T.-H. Hsu, Y.-H. Hsiao, S.-C. Lai, E.-K. Lai, S.-P. Hong, M.-T. Wu, F. H. Hsu, N. Z. Lien, C.-P. Lu, S.-Y. Wang, J.-Y. Hsieh, L.-W. Yang, T. Yang, K.-C. Chen, K.-Y. Hsieh, R. Liu, and C.-Y. Lu, "Understanding STI edge fringing field effect on the scaling of charge-trapping (CT) NAND flash and modeling of incremental step pulse programming (ISPP)," in *IEDM Tech. Dig.*, 2009, pp. 839–842.

[16] N. Sano, K. Matsuzawa, M. Mukai, and N. Nakayama, "On discrete random dopant modelling in drift–diffusion simulations: Physical meaning of 'atomistic' dopants," *Microelectron. Reliab.*, vol. 42, no. 2, pp. 189–199, Feb. 2002.

[17] A. Asenov, A. R. Brown, J. H. Davies, S. Kaya, and G. Slavcheva, "Simulation of intrinsic parameter fluctuations in decananometer and nanometer-scale MOSFETs," *IEEE Trans. Electron Devices*, vol. 50, no. 9, pp. 1837–1852, Sep. 2003.

[18] G. Roy, A. R. Brown, F. Adamu-Lema, S. Roy, and A. Asenov, "Simulation study of individual and combined sources of intrinsic parameter fluctuations in conventional Nano-MOSFETs," *IEEE Trans. Electron Devices*, vol. 52, no. 12, pp. 3063–3070, May 2006.

[19] M. F. Bukhori, S. Roy, and A. Asenov, "Statistical aspects of reliability in bulk MOSFETs with multiple defect states and random discrete dopants," *Microelectron. Reliab.*, vol. 48, no. 8/9, pp. 1549–1552, Aug./Sep. 2008.

[20] A. Ghetti, C. Monzio Compagnoni, A. S. Spinelli, and A. Visconti, "Comprehensive analysis of random telegraph noise instability and its scaling in deca-nanometer flash memories," *IEEE Trans. Electron Devices*, vol. 56, no. 8, pp. 1746–1752, Aug. 2009.

[21] Synopsys, Mountain View, CA, Sentaurus Device User Guide, 03 ed., 2007.

[22] A. Asenov, A. R. Brown, J. H. Davies, and S. Saini, "Hierarchical approach to 'atomistic' 3-D MOSFET simulation," *IEEE Trans. Comput.-Aided Design Integr. Circuits Syst.*, vol. 18, no. 11, pp. 1558–1565, Nov. 1999.

[23] A. Ghetti, C. Monzio Compagnoni, F. Biancardi, A. L. Lacaita, S. Beltrami, L. Chiavarone, A. S. Spinelli, and A. Visconti, "Scaling trends for random telegraph noise in deca-nanometer flash memories," in *IEDM Tech. Dig.*, 2008, pp. 835–838.

[24] A. Ghetti, M. Bonanomi, C. Monzio Compagnoni, A. S. Spinelli, A. L. Lacaita, and A. Visconti, "Physical modeling of single-trap RTS statistical distribution in flash memories," in *Proc. IRPS*, 2008, pp. 610–615.

[25] K. Sonoda, K. Ishikawa, T. Eimori, and O. Tsuchiya, "Discrete dopant effects on statistical variation of random telegraph signal magnitude," *IEEE Trans. Electron Devices*, vol. 54, no. 8, pp. 1918–1925, Aug. 2007.

[26] A. Asenov, R. Balasubramaniam, A. R. Brown, J. H. Davies, and S. Saini, "Random telegraph signal amplitudes in sub 100 nm (decanano) MOSFETs: A 3d 'atomistic' simulation study," in *IEDM Tech. Dig.*, 2000, pp. 279–282.

[27] C. Monzio Compagnoni, A. S. Spinelli, R. Gusmeroli, S. Beltrami, A. Ghetti, and A. Visconti, "Ultimate accuracy for the NAND flash program algorithm due to the electron injection statistics," *IEEE Trans. Electron Devices*, vol. 55, no. 10, pp. 2695–2702, Oct. 2008.
[28] C. Monzio Compagnoni, R. Gusmeroli, A. S. Spinelli, and A. Visconti, "Analytical model for the electron-injection statistics during programming of nanoscale NAND flash memories," *IEEE Trans. Electron Devices*, vol. 55, no. 11, pp. 3192–3199, Nov. 2008.
[29] H. Kurata, K. Otsuga, A. Kotabe, S. Kajiyama, T. Osabe, Y. Sasago, S. Narumi, K. Tokami, S. Kamohara, and O. Tsuchiya, "The impact of random telegraph signals on the scaling of multilevel flash memories," in *Proc. Symp. VLSI Circuits Dig.*, 2006, pp. 140–141.
[30] C. Monzio Compagnoni, R. Gusmeroli, A. S. Spinelli, A. L. Lacaita, M. Bonanomi, and A. Visconti, "Statistical model for random telegraph noise in flash memories," *IEEE Trans. Electron Devices*, vol. 55, no. 1, pp. 388–395, Jan. 2008.
[31] C. Monzio Compagnoni, M. Ghidotti, A. L. Lacaita, A. S. Spinelli, and A. Visconti, "Random telegraph noise effect on the programmed threshold-voltage distribution of flash memories," *IEEE Electron Device Lett.*, vol. 30, no. 9, pp. 984–986, Sep. 2009.
[32] H. H. Mueller and M. Schulz, "Random telegraph signal: An atomic probe of the local current in field-effect transistors," *J. Appl. Phys.*, vol. 83, no. 3, pp. 1734–1741, Feb. 1998.
[33] A. Asenov, R. Balasubramaniam, A. R. Brown, and J. H. Davies, "RTS amplitudes in decananometer MOSFETs: 3-D simulation study," *IEEE Trans. Electron Devices*, vol. 50, no. 3, pp. 839–845, Mar. 2003.

Aurelio Mauri was born in 1969. He received the M.S. degree (*cum laude*) in plasma physics from the University of Milan, Milano, Italy, in 1995.

He spent a research period at the Rutherford Appleton Laboratory, England, and at ENEA Frascati, Italy, on characterization and modeling of high-dense plasmas produced by laser confinement. In 1996, he worked for a semiconductor company focused on chemistry treatment of silicon surfaces. From 1998 to 2000, he spent a "nonworking" time helping the young generation. After that period, he came back to the semiconductor industries (STMicroelectronics) in the development of power devices. In 2004, he joined the nonvolatile technology development of the TCAD Group, STMicroelectronics, working in particular on NOR/NAND memories. He is currently with Numonyx, Agrate Brianza, Italy. He is the coauthor of more than 20 scientific conferences/papers on different physics topics.

Christian Monzio Compagnoni (M'08) was born in Busto Arsizio, Italy, in 1976. He received the Laurea degree (*cum laude*) in electronics engineering and the Ph.D. degree in information technology from Politecnico di Milano, Milano, Italy, in 2001 and 2005, respectively.

Since 2002, he has been with the Dipartimento di Elettronica e Informazione, Politecnico di Milano, where he became an Assistant Professor in 2006. He is also currently with the Italian University Nanoelectronics Team, Politecnico di Milano. His research interests include characterization and modeling of advanced nonvolatile memories and metal–oxide–semiconductor devices.

Dr. Monzio Compagnoni was a member of the memory committee of the IRPS in 2009 and 2010. He was the recipient of the Outstanding Paper Award at the IRPS in 2008.

Salvatore Maria Amoroso was born in Catania, Italy, in 1983. He received the B.S. and M.S. degrees in physics engineering from Politecnico di Milano, Milano, Italy, in 2005 and 2008, respectively, where he is currently working toward the Ph.D. degree in information technology.

In 2009, he joined the Dipartimento di Elettronica e Informazione, Politecnico di Milano. His research activities include modeling and numerical simulation of semiconductor devices, with particular interest on innovative nonvolatile memories.

Alessandro Maconi was born in Carate Brianza, Italy, in 1983. He received the Laurea degree in electronics engineering from Politecnico di Milano, Milano, Italy, in 2008, where he is currently working toward the Ph.D. degree.

In 2009, he joined the Dipartimento di Elettronica e Informazione, Politecnico di Milano. His research activities mainly involve characterization and modeling of advanced nonvolatile memories, with particular interests to TANOS memories.

Andrea Ghetti (M'98) was born in Forlì Italy, in 1968. He received the Laurea degree (*summa cum laude*) and Ph.D. degree in electrical engineering from the University of Bologna, Bologna, Italy, in 1994 and 1998, respectively.

In 1994, he was a Visiting Scientist with the TCAD Department, Intel Corporation, Santa Clara, CA. From March 1997 to March 2000, he held a postdoctoral position with Lucent Technologies, Bell Laboratories, Murray Hill, NJ. In May 2000, he joined STMicroelectronics, Agrate Brianza, Italy, which later became Numonyx, R&D—Technology Development, Agrate Brianza, where he is currently a Member of Technical Staff. He has authored or coauthored more than 80 peer-reviewed publications on international journals and conference proceedings. He also has coauthored a book on *Oxide Reliability* and has served in the IEDM Modeling and Simulation subcommittee. His research interests are in the field of nonvolatile memory development and device modeling, simulation and characterization with particular regard to 3-D effects, Monte Carlo simulation, quantum phenomena, mechanical stress, hot carrier, tunneling in MOS structures, gate oxide and array level reliability, RTN, and Phase Change Memory.

Dr. Ghetti received twice the "Outstanding paper award" at the International Reliability Physics Symposium in 2000 and 2008.

Alessandro S. Spinelli (M'99–SM'07) was born in Bergamo, Italy, in 1966. He received the Laurea (*cum laude*) and Ph.D. degrees in electronics engineering from Politecnico di Milano, Milano, Italy.

In 1995, he was a Visiting Scholar with The University of Tennessee Space Institute, Tullahoma, where he worked on single-molecule detection in a solution, and in 1996, he was a Consultant with the Central Department of Research and Development, STMicroelectronics, Agrate Brianza, Italy. In 1997, he became an Assistant Professor with Politecnico di Milano, and in 1998, he was an Associate Professor of electronics with the Università degli Studi dell'Insubria, Como, Italy. In 2001, he was a Visiting Professor with the Institut National Polytechnique de Grenoble, Grenoble, France. He is currently a Full Professor of electronics with Politecnico di Milano. He is also currently with the Italian University Nanoelectronics Team, Politecnico di Milano, and with the Istituto di Fotonica e Nanotecnologie, Consiglio Nazionale delle Ricerche, Milano. He has conducted experimental and theoretical research in electronics instrumentation and microelectronics, coauthoring more than 100 papers published in international journals or presented at international conferences. His current research interests include experimental characterization and modeling of nonvolatile memory cell reliability, development of innovative nonvolatile memories, and circuit design for biological signal readout.

Dr. Spinelli has served in the technical committees of the IEDM and IRPS conferences.

Andrea L. Lacaita (F'09) was born in 1962. He received the Laurea degree in nuclear engineering from Politecnico di Milano, Milano, Italy, in 1985.

From 1987 to 1992, he was a Researcher with the Consiglio Nazionale delle Ricerche (CNR), Milano. He was a Visiting Scientist/Professor with the AT&T Bell Laboratories, Murray Hill, NJ, from 1989 to 1990 and the IBM T. J. Watson Research Center, Yorktown Heights, NY, in 1999. Since 1992, he has been an EE Professor with Politecnico di Milano, where he became a Full Professor of electronics in 2000 and is currently teaching "Electron Devices" and "Electronic Circuit Design." Since 1992, he has also been the Head of the Micro and Nanoelectronics Laboratory, Dipartimento di Elettronica e Informazione, Politecnico di Milano. He served as Department Chair of the Dipartimento di Elettronica ad Informazione from 2006 to 2008 and Member of the Academic Senate from 2007 to 2008. He is also with the Italian University Nanoelectronics Team, Politecnico di Milano, and with the Istituto di Fotonica e Nanotecnologie, CNR. In the field of device physics, he has contributed to study in quantum effects, as well as experimental characterization techniques and numerical models of nonvolatile memories, both Flash and emerging (PCM and RRAM). He is the coauthor of more than 200 papers published in international journals or presented to international conferences, patents, and several educational books in electronics.

Prof. Lacaita served in several scientific committees such as IEEE IEDM (2001–2002), ESSDERC (2005), and IEEE VLSI Symposium (2005–2008). He was the IEDM European Chair from 2003 to 2004.